Available online at www.sciencedirect.com
ScienceDirect
Journal of Fluorine Chemistry 128 (2007) 1104–1111
JOURNAL OF FLUORINE CHEMISTRY
www.elsevier.com/locate/fluor

Preparation of fluoroalkyl end-capped oligomers/magnetite nanocomposites possessing a good dispersibility and stability

Hiroaki Yoshioka [a], Kei-Ichi Ohnishi [b], Hideo Sawada [a,*]

[a] *Department of Frontier Materials Chemistry, Faculty of Science and Technology, Hirosaki University Bunkyo-cho, Hirosaki 036-8561, Japan*
[b] *Asahi Glass Co. Ltd., Yurakucho, Chiyoda-ku, Tokyo 100-8405, Japan*

Received 6 March 2007; received in revised form 16 March 2007; accepted 19 March 2007
Available online 27 March 2007

Abstract

Fluoroalkyl end-capped vinylphosphonic acid cooligomers-encapsulated magnetite nanocomposites were prepared by the magnetization of aqueous ferric and ferrous ions in the presence of the corresponding fluorinated cooligomers and magnetic nanoparticles under alkaline conditions. These fluorinated cooligomers magnetic composites are nanometer size-controlled very fine particles and have a good dispersibility and stability in water and traditional organic solvents. These fluorinated nanocomposites were also applied to the surface modification of poly(methyl methacrylate) to exhibit a good oleophobicity imparted by fluorine on their surface. Fluoroalkyl end-capped 2-methacryloyloxyethanesulfonic acid oligomer-encapsulated magnetite nanocomposites and fluoroalkyl end-capped 2-acrylamide-2-methylpropanesulfonic acid oligomer-encapsulated magnetite nanocomposites were prepared in good isolated yields by the magnetization of iron chlorides in the presence of the corresponding oligomers and magnetic nanoparticles under similar conditions. Colloidal stability of these fluorinated nanocomposites thus obtained in water was demonstrated to become extremely higher than that of fluorinated vinylphosphonic acid cooligomers/magnetic nanocomposites.

Keywords: Fluorinated oligomer; Magnetite; Magnetic nanocomposite; Dispersibility; Stability; Surface dispersion; Polymer film

1. Introduction

There has been a great interest in well dispersed magnetic particles from the viewpoints of the applications in a wide variety of fields such as ferrofluids, high-density data storage, disks and toner in printing, magnetic resonance imaging (MRI), enzyme immobilization, bioseparation, drug delivery, immunoassays, and biosensors [1–11]. The surface functionality of magnetic nanoparticles by the use of functionalized polymers can afford the stable colloidal suspensions [12]. In fact, numerous synthetic and natural polymers have been used in order to obtain the stable colloidal dispersion of magnetic nanoparticles through the coating and encapsulation of the particles [13–20]. On the other hand, considerable interest has been devoted in recent years to block copolymers containing fluoroalkyl groups owing to exhibiting the low surface energy and the self-assembled polymeric aggregates resembling micelle in aqueous and organic media, which cannot be achieved in the corresponding randomly fluoroalkylated copolymers [21–23]. In these fluorinated polymers, we have already reported that ABA triblock-type fluoroalkyl end-capped oligomers can form the nanometer size-controlled self-assembled molecular aggregates with the aggregation of terminal fluoroalkyl segments in aqueous and organic media, and these fluorinated oligomeric aggregates could provide suitable host moieties to interact with a variety of guest molecules such as fullerenes, carbon nanotubes, and nanodiamonds [24,25]. From the developmental viewpoint of tailored magnetic polymer colloids possessing a good dispersibility and stability, it is in particular interest to develop the colloidal stable magnetic nanoparticles by the use of these fluoroalkyl end-capped oligomers. Recently, we developed a novel fluoroalkyl end-capped acrylic acid oligomers-encapsulated magnetite nanocomposites; however, colloidal stability of these fluorinated nanocomposites are extremely poor [26]. Hitherto, it is well known that utilizing the interaction between the hydroxyl

* Corresponding author. Tel.: +81 172 39 3578; fax: +81 172 39 3541.
E-mail address: hideosaw@cc.hirosaki-u.ac.jp (H. Sawada).

0022-1139/$ – see front matter © 2007 Elsevier B.V. All rights reserved.
doi:10.1016/j.jfluchem.2007.03.016

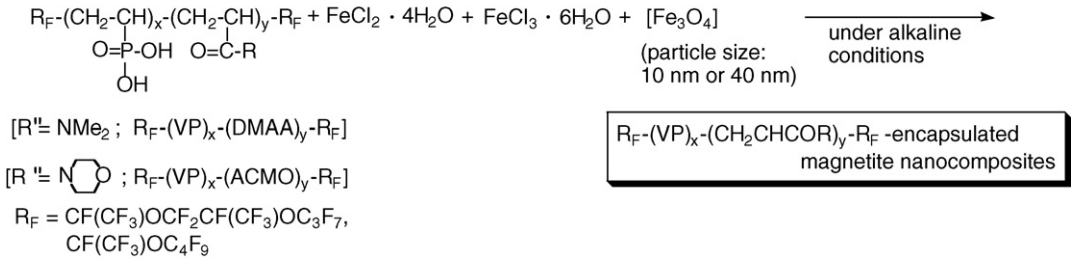

Scheme 1.

groups in metal and the phosphonic acid groups is a promising approach to the surface modification of metal oxide nanoparticles [27,28]. Therefore, it is strongly expected that fluoroalkyl end-capped oligomers containing not only phosphonic acid groups but also other functional groups such as sulfonic acid and sulfobetaine-type groups should interact strongly with the hydroxyl groups on the magnetic surface to afford new fluorinated magnetic nanocomposites with a good dispersibility and stability in a variety of solvents including water. In our comprehensive studies on the developments of new fluorinated metal nanoparticles, we have found that these fluoroalkyl end-capped oligomers are convenient tools for the preparation of colloidal stable magnetic particles in a variety of solvents. These results will be described herein.

2. Results and discussion

Fluoroalkyl end-capped vinylphosphonic acid cooligomers [R_F-$(VP)_x$-$(CH_2CHCOR)_y$-R_F] reacted with aqueous Fe^{3+} and Fe^{2+} ions under alkaline conditions to afford R_F-$(VP)_x$-$(CH_2CHCOR)_y$-R_F/magnetite nanocomposites in good isolated yields. We have also succeeded in preparing R_F-$(VP)_x$-$(CH_2CHCOR)_y$-R_F/Fe_3O_4/magnetic nanocomposites by the coprecipitations of iron chlorides in the presence of magnetic nanoparticles (mean diameters: 10 and 40 nm) under similar conditions. These results were also shown in Scheme 1 and Table 1.

The dynamic light scattering (DLS) measurements at 30 °C showed that the size (number-average diameter) of molecular assemblies formed in aqueous solutions of R_F-$(VP)_x$-$(DMAA)_y$-R_F and R_F-$(VP)_x$-$(ACMO)_y$-R_F cooligomers could increase from 16–126 to 57–516 nm by the magnetization of the fluorinated cooligomers with iron ions. The significant increase of the aggregate size in fluorinated cooligomers suggests that the original magnetic nanoparticles and magnetic particles, which can be prepared from the coprecipitation of aqueous iron ions under alkaline conditions, should be encapsulated effectively into fluorinated cooligomeric aggregates cores formed by the aggregation of terminal fluoroalkyl groups in cooligomers through the strong interactions between the magnetite-OH and phosphonic acid segments in cooligomers.

The contents of fluorinated cooligomers in nanocomposites were estimated by the use of TGA, in which the weight loss of these nanocomposites were measured by raising the temperature around to 800 °C, and the results were shown in Fig. 1 and Table 2.

Table 1
Reactions of fluoroalkyl end-capped VP cooligomers with ferric and ferrous chloride in the presence of magnetic nanoparticles under alkaline conditions

Run	R_F-Oligomer [x:y][a](mg)	Fe_3O_4 (mg)	$FeCl_2{\cdot}4H_2O$ (mmol)	$FeCl_3{\cdot}6H_2O$ (mmol)	Yield (%)[b]	Particle size[c] (nm)
R_F-$(VP)_x$-$(DMAA)_y$-R_F[R_F = $CF(CF_3)OCF_2CF(CF_3)OC_3F_7$]						
1	[11:89] (40)	100[d]	1.5	2.7	91	189.2 ± 39.3 [18.8 ± 3.7][e]
2	[11:89] (40)	75[d]	1.5	2.7	95	167.1 ± 35.7
3	[11:89] (40)	50[d]	1.5	2.7	77	112.7 ± 25.4
4	[11:89] (40)	25[d]	1.5	2.7	82	164.3 ± 32.0
5	[11:89] (20)	0	1.5	2.7	96	420.4 ± 80.4
R_F-$(VP)_x$-$(ACMO)_y$-R_F [R_F = $CF(CF_3)OCF_2CF(CF_3)OC_3F_7$]						
6	[34:66] (20)	0	1.5	2.7	96	308.5 ± 44.1 [16.1 ± 6.9][e]
R_F-$(VP)_x$-$(DMAA)_y$-R_F [R_F = $(3F(CF_3)OC_4F_9)$]						
7	[31:69] (40)	50[f]	1.5	2.7	87	57.2 ± 11.5 [10.6 ± 0.8]
8	[39:61] (40)	50[f]	1.5	2.7	83	139.3 ± 26.9 [26.0 ± 3.2][e]
9	[46:54] (40)	5[f]	1.5	2.7	79	515.8 ± 96.0 [126.4 ± 13.7][e]

[a] Cooligomerization ratio (x:y) was determined by ^{1}H NMR.
[b] Yield was based on fluorinated cooligomer, Fe_3O_4 derived from the coprecipitation of $FeCl_2$ and $FeCl_3$ under alkaline conditions, and the used original Fe_3O_4 nanoparticle.
[c] Number average particle size in water determined by dynamic light scattering measurements (DLS).
[d] 40 nm magnetic nanoparticle was used.
[e] Number average particle size of parent fluorinated cooligomer determined by DLS.
[f] 10 nm magnetic nanoparticle was used.

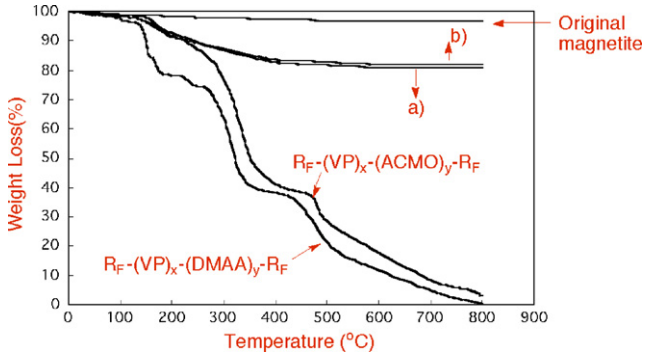

Fig. 1. Thermogravimetric analyses of R_F-(VP)$_x$-(DMAA)$_y$-R_F-magnetite nanocomposites [(b): Run 5 in Table 1], R_F-(VP)$_x$-(ACMO)$_y$-R_F-magnetite nanocomposites [(a): Run 6 in Table 1], R_F-(VP)$_x$-(DMAA)$_y$-R_F, R_F-(VP)$_x$-(ACMO)$_y$-R_F, and original magnetite [R_F = CF(CF$_3$)OCF$_2$CF(CF$_3$)OC$_3$F$_7$].

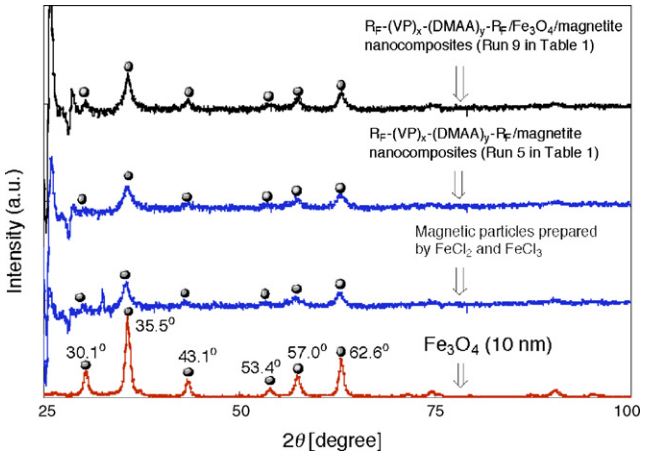

Fig. 2. X-ray diffractions of Fe_3O_4 and fluoroalkyl end-capped VP cooligomers-encapsulated magnetite nanocomposites.

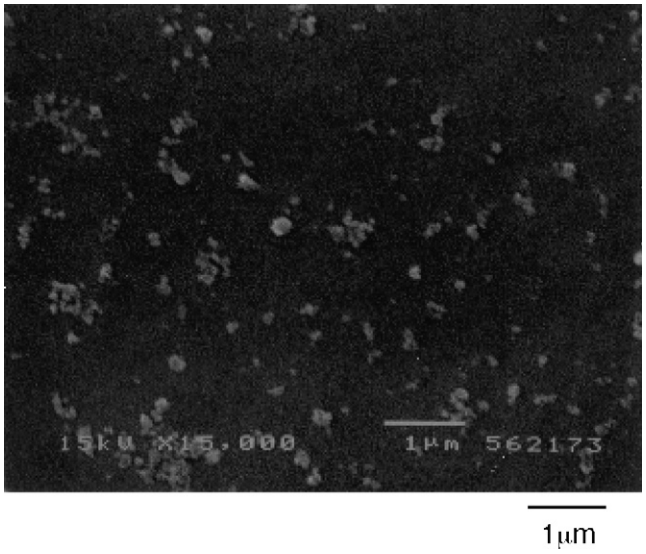

Fig. 3. SEM images of R_F-(VP)$_x$-(DMAA)$_y$-R_F/Fe$_3$O$_4$/magnetite nanocomposites [R_F = CF(CF$_3$)OC$_4$F$_9$: Run 9 in Table 1].

As shown in Fig. 1, thermal stability: T_{dec} (defined by a 10% mass loss at a 10 °C/min heating rate) of fluorinated cooligomers was found to decrease effectively, compared to that of the corresponding nanocomposites. The contents of fluorinated cooligomeric segments in the composites were estimated to be 15–16% by the use of the TGA data for the thermal stabilities of the parent magnetite, fluorinated cooligomers and the fluorinated cooligomeric nanocomposites. The contents (11–19%) of fluorinated cooligomers in other composites were estimated by the use of TGA measurements under similar conditions (see Table 2).

As shown in Fig. 2, XRD patterns of our present fluorinated VP cooligomer/Fe_3O_4/magnetite nanocomposites and fluorinated VP cooligomer/magnetite nanocomposites exhibit a similar characteristic to that of the parent magnetite or magnetic particles prepared by $FeCl_2$ and $FeCl_3$ under alkaline conditions. This finding indicates the presence of magnetites in our fluorinated nanocomposites.

Fig. 3 shows the typical scanning electron microscopy (SEM) micrograph for R_F-(VP)$_x$-(DMAA)$_y$-R_F/Fe$_3$O$_4$/magnetite nanocomposites [R_F = CF(CF$_3$)OC$_4$F$_9$]. They were essentially very fine particles and were controlled with nanometer-size levels (mean: 183 nm).

Table 2
Thermal stability (T_{dec})[a] of R_F-(VP)$_x$-(CH$_2$CHCOR)$_y$-R_F-encapsulated magnetite nanocomposites and the contents of R_F-(VP)$_x$-(CH$_2$CHCOR)$_y$-R_F in nanocomposites

Run[b]	Fluorinated nanocomposite	T_{dec} (°C)	Content of cooligomer in composite (%)[c]
1	R_F-(VP)$_x$-(DMAA)$_y$-R_F/Fe$_3$O$_4$/magnetite nanocomposite [R_F = CF(CF$_3$)OCF$_2$CF(CF3)OC$_3$F$_7$]	294 [226][d]	15
2		234	11
3		332	19
4		279	13
5	R_F-(VP)$_x$-(DMAA)$_y$-R_F/magnetite nanocomposite [R_F = CF(CF$_3$)OCF$_2$CF(CF$_3$)OC$_3$F$_7$]	242 [226][d]	15
6	R_F-(VP)$_x$-(ACMO)$_y$-R_F/magnetite nanocomposite [R_F = CF(CF$_3$)OCF$_2$CF(CF$_3$)OC$_3$F$_7$]	234 [121][d]	16
7	R_F-(VP)$_x$-(DMAA)$_y$-R_F/Fe$_3$0$_4$/magnetite nanocomposite [R_F = CF(CF$_3$)OC$_4$F$_9$]	256 [174][d]	18
8		251 [196][d]	18
9		272 [204][d]	18

[a] Defined by a 10% mass loss at a 10 °C/min heating rate.
[b] Each different from those of Table 1.
[c] Contents of fluorinated oligomers in nanocomposites determined by TGA.
[d] Parent fluorinated cooligomer.

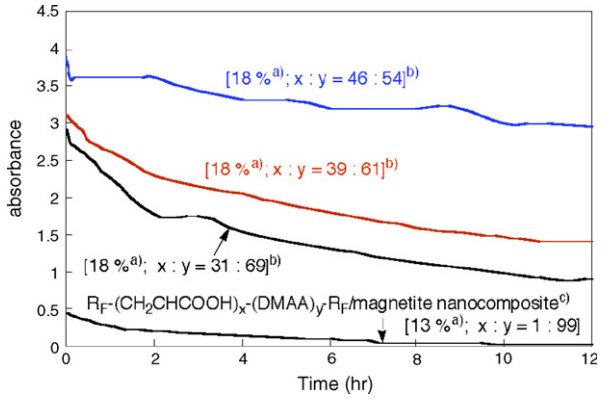

Fig. 4. UV–vis spectral changes of the absorption at λ = 500 nm of aqueous solutions in the presence of R_F-(VP)$_x$-(DMAA)$_y$-R_F/Fe_3O_4/magnetite nanocomposite [R_F = $CF(CF_3)OC_4F_9$] as a function of time at 30 °C. (a) Contents of fluorinated oligomers in composite determined by TGA. (b) Cooligomerization ratio in cooligomer determined by ^{1}H NMR. (c) R_F = $CF(CF_3)OCF_2CF(CF3)OC_3F_7$.

We have studied on the colloidal stabilization of our present fluorinated vinylphosphonic acid cooligomer-encapsulated magnetite nanoparticles in aqueous and organic media. The colloidal suspensions of these fluorinated nanocomposites in water and organic solvents such as chloroform, tetrahydrofuran and methanol are stable without the separation over 12 h at room temperature, respectively, although the colloidal suspensions of our previously reported R_F-$(CH_2CHCOOH)_x$-$(CH_2CHCONMe_2)_y$-R_F/magnetite nanocomposites [26] have an extremely poor colloidal stability in these media.

We have tested the aqueous solutions containing fluorinated oligomers-encapsulated magnetite nanocomposites for the dispersibility and stability by the use of UV–vis spectra at 30 °C, and the results were shown in Fig. 4.

Fig. 4 shows the UV–vis spectra changes of the absorbance at λ = 500 nm of aqueous solutions containing fluoroalkyl end-capped oligomers-encapsulated magnetite colloidal particles as a function of time. It was demonstrated that our present fluorinated cooligomers-encapsulated magnetite colloidal particles (concentration of each nanocomposite: 0.2 g/dm^3) are well dispersed in aqueous solutions with a good stability, compared to that of the acrylic acid cooligomer/magnetite nanoparticles (concentration of this nanocomposite: 0.2 g/dm^3). More interestingly, the contents of vinylphosphonic acid segments in fluorinated cooligomers become higher from 31 to 46%, the colloidal stability of fluorinated magnetites was found to become higher. A higher colloidal stability of fluorinated VP cooligomers-encapsulated magnetite nanocomposites, compared to that of fluorinated acrylic acid cooligomer/magnetite nanocomposites, would be due to the stronger hydrogen bonding interaction between the vinylphosphonic acid segments in fluoroalkylated cooligomers onto residual hydroxy groups in magnetic nanoparticles.

In this way, our present fluorinated VP cooligomers magnetic composites are nanometer-size controlled fine particles, and have a good dispersibility in a variety of organic media. Thus, it is in particular interest to apply our fluorinated nanocomposites to the surface modification of traditional organic polymers such as poly(methyl methacrylate) (PMMA). We have prepared the modified PMMA film by casting the homogeneous tetrahydrofuran solution containing PMMA, fluorinated VP-DMAA cooligomer [R_F = $CF(CF_3)OC_4F_9$; *x*:*y* = 46:54] and iron chlorides. The obtained dark-yellow PMMA film (film thickness: 218 μm) was immersed in an aqueous ammonia solution (pH 10), and this ammonia solution was then stirred for 5 h at room temperature. During stirring, the color of the film surface changed from the dark-yellow to the black. The FT-IR spectrum peak around 580 cm^{-1} in this modified PMMA film reveals the presence of Fe_3O_4 in the modified film. The contact angles of dodecane on the surface and reverse sides of the modified PMMA film treated with fluorinated oligomer-encapsulated magnetic nanoparticles are 40° and 14°, respectively. A higher value for the contact angle on the surface side suggests that fluorinated oligomer could be arranged on the polymer surface to exhibit a strong oleophobicity imparted by fluoroalkyl segments on the surface. The contact angle of dodecane on the modified PMMA film surface before the treatment with an aqueous ammonia solution was 44° (reverse side: 17°). Therefore, the large decrease of the contact angles of dodecane was not observed before and after the treatment of the polymer surface with aqueous ammonia solution. This finding suggests that fluoroalkyl end-capped cooligomer-encapsulated magnetite nanocomposites should be prepared on the PMMA film surface by covalently binding the phosphonic acid segments in hydrophilic fluorinated cooligomers onto the residual hydroxyl groups in magnetic particles, which were obtained by the magnetization on the polymer surface of iron chlorides with aqueous ammonia solutions.

From the developmental viewpoints of new fluorinated functional materials, it is very important to prepare the fluorinated oligomers-encapsulated magnetite nanocomposites possessing a higher colloidal dispersibility and stability into a variety of solvents. Thus, we tried to prepare new fluorinated oligomers containing sulfo and sulfobetaine-type segments-encapsulated magnetite nanocomposites, because these functional groups should have a higher covalently binding characteristic onto the residual hydroxyl groups in magnetic particles than that of vinylphosphonic acid segments in

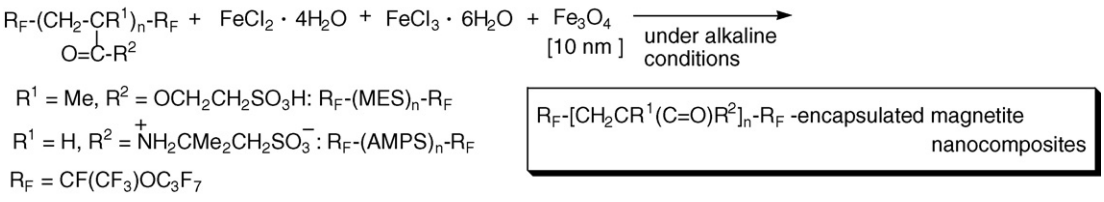

Scheme 2.

Table 3
Reactions of ferric chloride and ferrous chloride in the presence of fluoroalkyl end-capped MES and AMPS oligomers under alkaline conditions

Run	oligomer (mg)	Fe_3O_4 (size: 10 nm) (mg)	$FeCl_2 \cdot 4H_2O$ (mmol)	$FeCl_3 \cdot 6H_2O$ (mmol)	Yield (%)[a]	Particle size[b] (nm)	T_{dec} (°C)[c]	Content of oligomer in composite (%)[d]
R_F-$(MES)_n$-R_F								
1	40	0	1.5	2.7	86	58.6 ± 9.9 [10.4 ± 0.7][e]	249	22
2	40	25	1.5	2.7	89	99.0 ± 2.5	298	14
3	40	50	1.5	2.7	92	39.7 ± 8.2	309	13
R_F-$(AMPS)_n$-R_F								
4	40	0	1.5	2.7	87	56.5 ± 8.7[f]	204	27
5	40	25	1.5	2.7	91	95.0 ± 2.0	241	17
6	40	50	1.5	2.7	96	155.4 ± 34.5	294	15

[a] Yield was based on oligomer, and Fe_3O_4 derived from the coprecipitation of $FeCl_2$ and $FeCl_3$ under alkaline conditions.
[b] Number average particle size in water determined by dynamic light scattering measurements.
[c] Defined by a 10% mass loss at a 10 °C/min heating rate in TGA measurements.
[d] Contents of fluorinated oligomers in nanocomposites determined by TGA.
[e] Number average particle size of parent fluorinated cooligomer.
[f] Particle size of the parent fluorinated AMPS oligomer was not determined due to the gelling characteristic in water.

fluorinated cooligomers. In fact, as shown in Scheme 2 and Table 3, we have succeeded in preparing new fluoroalkyl end-capped 2-methacryloyloxyethanesulfonic acid oligomer [R_F-$(MES)_n$-R_F]-encapsulated magnetite nanocomposites and fluoroalkyl end-capped 2-acrylamide-2-methylpropanesulfonic acid oligomer [R_F-$(AMPS)_n$-R_F]-encapsulated magnetite nanocomposites in good isolated yields (86–96%) under similar conditions as that of Scheme 1. DLS measurements showed that the size (number-average diameter) of R_F-$(MES)_n$-R_F-encapsulated magnetite nanocomposites increased from 10 to 40–99 nm by the magnetization of R_F-$(MES)_n$-R_F with ferrous and ferric ions. The increase of the size of magnetic nanoparticles indicates that magnetic nanoparticles should be tightly encapsulated into the self-assembled fluorinated oligomeric aggregates formed by the aggregation of end-capped fluoroalkyl segments in R_F-$(MES)_n$-R_F oligomer to afford fine fluorinated MES oligomer magnetic nanocomposites. Similarly, nanometer size-controlled R_F-$(AMPS)_n$-R_F-encapsulated magnetite nanocomposites (particle size: 57–155 nm) were obtained by the magnetization of R_F-$(AMPS)_n$-R_F with ferrous and ferric ions under alkaline conditions in the presence (or the absence) of magnetic nanoparticles.

The contents of fluorinated MES and AMPS oligomers in the magnetic nanocomposites were estimated to be 13–27% by the use of the TGA data for the thermal stabilities of the parent magnetic nanoparticles, fluorinated MES, AMPS oligomers, and the fluorinated oligomeric nanocomposites (see Table 3).

Fig. 5 shows the typical TEM micrograph for R_F-$(MES)_n$-R_F [$R_F = CF(CF_3)OC_3F_7$]-encapsulated magnetic primary nanoparticles (mean diameter: 19 nm). They were essentially very fine and were controlled with nanometer-size levels.

XRD patterns of R_F-$(MES)_n$-R_F/magnetite nanocomposites and R_F-$(AMPS)_n$-R_F/magnetite nanocomposites exhibit a similar characteristic to that of the parent magnetite, indicating the presence of magnetites in these fluorinated nanocomposites (see Fig. 6).

The colloidal suspensions of fluorinated MES and AMPS oligomers-encapsulated magnetite nanocomposites (concentration of each nanocomposite: 0.2 g/dm^3) in water, and organic solvents such as tetrahydrofuran are stable without the

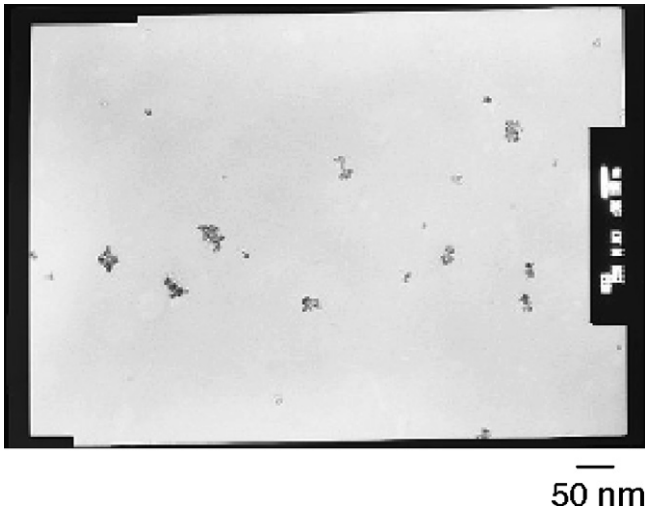

Fig. 5. TEM images of R_F-$(MES)_n$-R_F-encapsulated magnetite nanocomposites (Run 1 in Table 3).

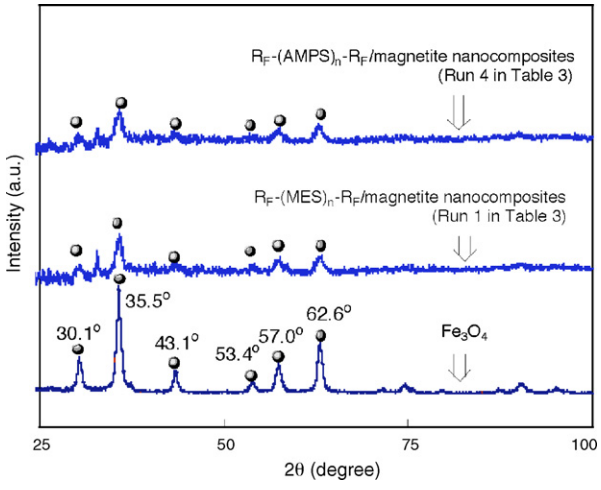

Fig. 6. X-ray diffraction of Fe_3O_4 and R_F-$(MES)_n$-R_F/magnetite nanocomposites and R_F-$(AMPS)_n$-R_F/magnetite nanocomposites.

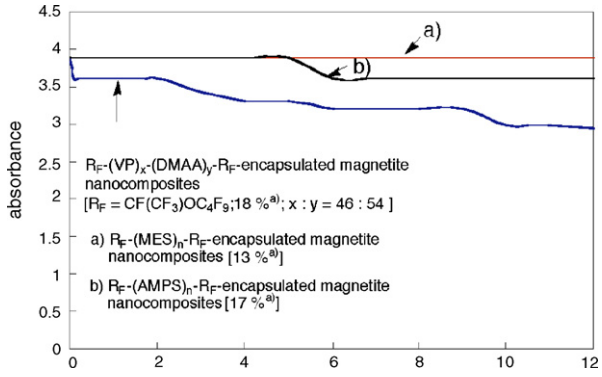

Fig. 7. UV–vis spectral changes of the absorption at λ = 500 nm of aqueous solutions in the presence of fluorinated oligomers magnetic nanocomposites as a function of time at 30 °C (a) content of oligomer in composites.

separation. The UV–vis spectra changes of the absorbance at λ = 500 nm of aqueous solutions containing R_F-(MES)$_n$-R_F-encapsulated magnetite nanocomposites and R_F-(AMPS)$_n$-R_F-encapsulated magnetite nanocomposites show that the colloidal stability of these nanocomposites is extremely higher than that of fluorinated vinylphosphonic acid cooligomeric magnetite nanoparticles (see Fig. 7). Especially, the dispersibility and stability of R_F-(MES)$_n$-R_F-encapsulated magnetite nanocomposites became extraordinary higher. This would be due to the strong interaction between the sulfo segments and the magnetite surface.

To investigate the magnetic response against an external magnetic field, UV–vis spectra were measured as a function of time after the permanent magnet was applied from the bottom of the cell (see Figs. 8 and 9).

As shown in Figs. 8 and 9, R_F-(MES)$_n$-R_F-encapsulated magnetite nanocomposites and R_F-(AMPS)$_n$-R_F-encapsulated magnetite nanocomposites exhibited a good dispersibility and stability in water; however the absorbance extremely decreased in water by applying the magnet. This finding indicates that the fluorinated magnetic nanocomposites still maintain their ferromagnetism.

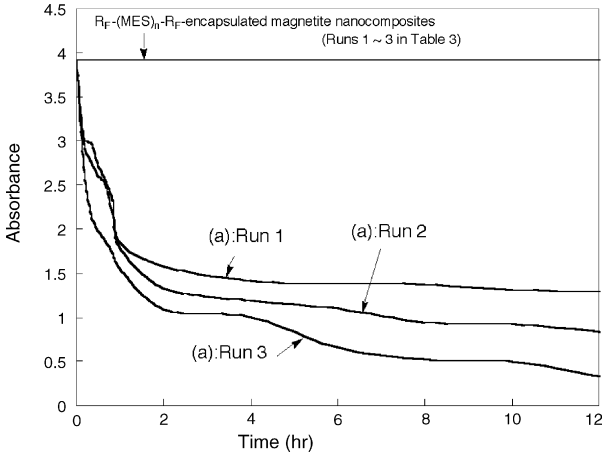

Fig. 8. UV–vis spectral changes of the absorption at λ = 500 nm of aqueous solutions in the presence of R_F-(MES)$_n$-R_F-encapsulated magnetite nanocomposites (Runs 1–3 in Table 3) as a function of time 30 °C (a) absorbance from placing the magnet at the bottom of cell.

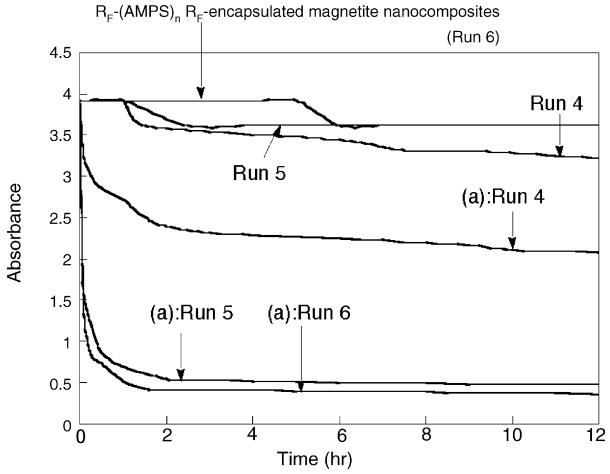

Fig. 9. UV–vis spectral changes of the absorption at λ = 500 nm of aqueous solutions in the presence of R_F-(AMPS)$_n$-R_F-encapsulated magnetic nanocomposites (Runs 4–6 in Table 3) as a function of time 30 °C (a) absorbance from placing the magnet at the bottom of cell.

In conclusion, we have succeeded in preparing fluoroalkyl end-capped VP cooligomers-encapsulated magnetite nanocomposites, fluoroalkyl end-capped MES oligomer-encapsulated magnetite nanocomposites, and fluoroalkyl end-capped AMPS oligomer-encapsulated magnetite nanocomposites by the magnetizations of ferric and ferrous ions in the presence of the corresponding fluorinated oligomers and magnetic nanoparticles under alkaline conditions. These fluorinated oligomers magnetic nanocomposites thus obtained are nanometer size-controlled fine particles, and the colloidal suspensions of these fluorinated nanocomposites in water and a variety of organic media are stable without the separation over 12 h at room temperature. Especially, the colloidal stability of fluorinated MES and AMPS oligomers-encapsulated magnetite nanocomposites in water is extremely higher than that of the corresponding fluorinated vinylphosphonic acid cooligomers-encapsulated magnetite nanocomposites. In particular interest, it was verified that the dispersibility and stability of fluorinated MES oligomer-encapsulated magnetite nanocomposites in water became extraordinary higher, compared to the other fluorinated oligomers magnetic nanocomposites. Therefore, our present fluorinated oligomers-encapsulated magnetite nanocomposites have high potential for new fluorinated polymeric functional materials possessing both surface active characteristic imparted by fluorine and magnetic property.

3. Experimental

3.1. Measurements

NMR spectra were measured using JEOL JNM-400 (400 MHz) FT NMR SYSTEM (Tokyo, Japan). Dynamic light-scattering (DLS) measurements were measured using Otsuka Electronics DLS-7000 HL (Tokyo, Japan). Thermal analyses were recorded on RIGAKUDENKI TG8101 D

differential thermobalance (Tokyo, Japan). Ultraviolet–visible (UV–vis) spectra were measured using Shimadzu UV-1600 UV–vis spectrophotometer (Kyoto, Japan). Molecular weights were measured using a Shodex DS-4 (pomp) and Shodex RI-71 (Detector) gel permeation chromatography (GPC) calibrated with standard poly(ethylene glycol) using 0.2 M Na_2HPO_4 solution as the eluent. Contact angles were measured by the use of the goniometer type contact angle meter (ERMA G-1-1000). The formation of the fluorinated oligomeric nanocomposites were observed from SEM (scanning electron microscope: JEOL JSM-5300, Tokyo, Japan) and TEM (transmission electron microscopy: JEOL JEM-1210 electron microscopy, Tokyo, Japan) images. Fourier-transform infrared (FTIR) spectra were measured using Shimadzu FTIR-8400 FT-IR spectrophotometer (Kyoto, Japan).

4. Materials

N,*N*-Dimethylacrylamide (DMAA) and acryloylmorpholine (ACMO) were used as received from Kohjin Co., Ltd. (Tokyo, Japan). 2-Acrylamide-2-methylpropanesulfonic acid (AMPS) and 2-methacryloyloxyethanesulfonic acid (MES) were used as received from Tokyo Kasei Kogyo Co., Ltd. (Tokyo, Japan) and NOF Corporation (Tokyo, Japan), respectively. Vinylphosphonic acid was purchased from the Sigma-Aldrich Japan Co., Ltd. (Tokyo, Japan). A variety of fluoroalkyl end-capped VP cooligomers, R_F-$(MES)_n$-R_F and R_F-$(AMPS)_n$-R_F oligomers were prepared by the reactions of fluoroalkanoyl peroxides with the corresponding monomers according to our previously reported methods [29–31].

4.1. A typical procedure for the preparation of fluorinated oligomers-encapsulated magnetite nanocomposites

To an aqueous solution containing $FeCl_2{\cdot}4H_2O$ (1.5 mmol), $FeCl_3{\cdot}6H_2O$ (2.7 mmol), and magnetic nanoparticles (40 nm: 100 mg) was added an aqueous solution (5 ml) of R_F-$(VP)_x$-$(DMAA)_y$-R_F; $R_F = CF(CF_3)OCF_2CF(CF3)OC_3F_7$ [M_n = 840 (molecular weight of this cooligomers is the apparent molecular weight due to the strong aggregate characteristic (M_w/M_n = 48) of this cooligomer in the eluent), 4 g/dm^3]. The mixture was sonicated for 30 min at room temperature, and was then made alkaline (pH 10) by the addition of 25% aqueous ammonia solution. The product was recovered by a permanent magnet and then washed with water to remove free oligomer. The obtained black material was dried at 50 °C in vacuo to afford fluoroalkyl end-capped VP cooligomer magnetic nanocomposites (411 mg). Other fluoroalkyl end-capped VP-DMAA cooligomers [$R_F = CF(CF_3)OC_4F_9$: M_n = 1980 (x:y = 31:69); $R_F = CF(CF_3)OC_4F_9$: M_n = 4230 (x:y = 39:61); $R_F = CF(CF_3)OC_4F_9$: M_n = 3050 (x:y = 46:54)], R_F-$(VP)_x$-$(ACMO)_y$-R_F [$R_F = CF(CF_3)OCF_2CF(CF_3)OC_3F_7$: M_n = 1490 (x:y = 34:66), R_F-$(MES)_n$-R_F oligomer [$R_F = CF(CF_3)OC_3F_7$; M_n = 12300], and R_F-$(AMPS)_n$-R_F oligomer [$R_F = CF(CF_3)OC_3F_7$; molecular weight was not determined due to gelling of the sample] magnetites nanocomposites were prepared under similar conditions.

4.2. Colloidal stability of fluorinated oligomers-encapsulated magnetite nanocomposites in a variety of solvents

In a 10 ml vial, 10 mg of fluorinated VP-DMAA cooligomers-encapsulated magnetite nanocomposites and 5 ml of water were mixed vigorously for 5 min at room temperature. After standing at room temperature, the separation time of this colloidal solution was measured.

4.3. Preparation of the modified PMMA film, and contact angle measurements

The PMMA film (film thickness: 218 μm) was prepared by casting the homogeneous tetrahydrofuran solution (32 ml) containing PMMA (1.0 g), R_F-$(VP)_x$-$(DMAA)_y$-R_F oligomer [$R_F = CF(CF_3)OC_4F_9$; x:y = 46:54; 10 mg], $FeCl_3{\cdot}6H_2O$ (9 mg), and $FeCl_2{\cdot}4H_2O$ (4 mg). The obtained dark-yellow PMMA film was immersed in an aqueous ammonia solution (pH 10), and this ammonia solution was then stirred for 5 h at room temperature. During stirring, the color of the film surface changed from the dark-yellow to the black. Contact angle measurements of dodecane on the obtained film were measured by the use of the goniometer type contact angle meter at room temperature.

Acknowledgments

The authors gratefully appreciate the financial support from a grant-in-aid for Scientific Research from the Ministry of Education, Science, Sports and Culture, Japan. The authors also thank to Toda Kogyo Corporation (Hiroshima, Japan), Kohjin Co., Ltd. (Tokyo, Japan), and NOF Corporation (Tokyo, Japan) for supply of magnetic nanoparticles (10 and 40 nm), DMAA, ACMO, and MES, respectively.

References

[1] S.H. Sun, C.B. Murray, D. Weller, L. Folks, A. Moser, Science 287 (2000) 1989–1992.
[2] S.H. Sun, H. Zeng, D.B. Robinson, S. Raoux, P.M. Rice, S.X. Wang, G. Li, J. Am. Chem. Soc. 126 (2004) 273–279.
[3] X.K. Gao, K.M.K. Yu, K.Y. Tam, S.C. Tsang, Chem. Commun. 24 (2003) 2998–2999.
[4] Y.C. Chang, D.H. Chen, J. Colloid Interface Sci. 283 (2005) 446–451.
[5] Y.C. Chang, D.H. Chen, Macromol. Biosci. 5 (2005) 254–261.
[6] M. Shimomura, N. Sugiyama, T. Yamauchi, S. Miyauchi, Polym. J. 30 (1998) 350–351.
[7] M. Shinkai, H. Honda, T. Kobayashi, Biocatalyst 5 (1991) 61–69.
[8] A. Millan, F. Palacio, Appl. Organomet. Chem. 15 (2001) 396–400.
[9] T.E. Karis, J. Appl. Polym. Sci. 59 (1996) 1405–1416.
[10] X. Li, Z. Sun, J. Appl. Polym. Sci. 58 (1995) 1991–1997.
[11] D.H. Chen, M.H. Liao, J. Mol. Catal. B: Enzym. 16 (2002) 283–291.
[12] S.-Y. Mak, D.-H. Chen, Macromol. Rapid Commun. 26 (2005) 1567–1571.
[13] C. Flesch, Y. Unterfinger, E. Bourgeat-Lami, E. Duguet, C. Delaite, P. Dumas, Macromol. Rapid Commun. 26 (2005) 1494–1498.
[14] G. Song, J. Bo, R. Guo, Colloid Polym. Sci. 282 (2004) 656–660.
[15] L. Dumazet-Bonnamour, P.L. Perchee, Colloid Surfaces A: Phys. Eng. Aspects 173 (2000) 61–71.

[16] B. Lindlar, M. Boldt, S. Eiden-Assmann, G. Maret, Adv. Mater. 14 (2002) 1656–1658.
[17] M. Kryszewski, J.K. Jeszka, Synth. Metals 94 (1998) 99–104.
[18] B.H. Sohn, R.E. Cohen, Chem. Mater. 9 (1997) 264–269.
[19] M.-H. Liao, K.-Y. Wu, D.-H. Chen, Chem. Lett. 32 (2003) 488–489.
[20] M.T. Nguyen, A.F. Diaz, Adv. Mater. 6 (1994) 858–860.
[21] J.-F. Berret, D. Calvet, A. Collet, M. Viguier, Curr. Opin. Colloid Interface Sci. 8 (2003) 296–306.
[22] T. Imae, Curr. Opin. Colloid Interface Sci. 8 (2003) 307–314.
[23] T. Imae, H. Tabuchi, K. Funayama, A. Sato, T. Nakamura, N. Amaya, Colloid Surf. A: Physicochem. Eng. Aspects 167 (2000) 73–81.
[24] H. Sawada, Prog. Polym., Sci., in press.
[25] H. Sawada, Polym. J., in press.
[26] H. Sawada, H. Yoshioka, T. Kawase, K. Ueno, K. Hamazaki, J. Fluorine Chem. 126 (2005) 914–917.
[27] J.G. Van Alsten, Langmuir 15 (1999) 7605–7614.
[28] C. Yee, G. Kataby, A. Ulman, T. Prozorov, H. White, A. King, M. Rafailovich, J. Sokolov, A. Gedanken, Langmuir 15 (1999) 7111–7115.
[29] H. Sawada, D. Tamada, T. Kawase, Y. Hayakawa, K. Lee, J. Kyokane, M. Baba, J. Appl. Polym. Sci. 79 (2001) 228–245.
[30] H. Sawada, A. Ohashi, M. Baba, T. Kawase, Y. Hayakawa, J. Fluorine Chem. 79 (1996) 149–155.
[31] H. Sawada, S. Katayama, Y. Ariyoshi, T. Kawase, Y. Hayakawa, T. Tomita, M. Baba, J. Mater. Chem. 8 (1998) 1517–1524.